

# HIGH RESOLUTION CARDIAC SHAPE REGISTRATION USING RICCI FLOW

Mingchen Gao<sup>1</sup>, Rui Shi<sup>2</sup>, Shaoting Zhang<sup>1</sup>, Wei Zeng<sup>3</sup>, Zhen Qian<sup>4</sup>,  
Xianfeng David Gu<sup>2</sup>, Dimitris Metaxas<sup>1</sup>, Leon Axel<sup>5</sup>

<sup>1</sup>CBIM, Rutgers University, Piscataway, NJ <sup>2</sup>Stony Brook University, Stony Brook, NY

<sup>3</sup>Florida International University, Miami, FL <sup>4</sup>Piedmont Heart Institute, Atlanta, GA

<sup>5</sup>New York University, 660 First Avenue, New York, NY

## ABSTRACT

Current CT techniques are able to produce isotropic high resolution CT images ( $0.5mm$ ). Recent research has revealed that the interior of the left ventricle has complex structures and topology, which has potentially valuable information. However, this makes the matching between models much more challenging. In this paper, we propose a novel method to match two models with non-trivial topology. 3D mesh models are flattened onto a 2D planar surfaces using discrete hyperbolic Ricci flow. Therefore, the 3D matching problem is converted to a much simpler 2D matching problem. We show the performance on the registration of high resolution left ventricle models.

*Index Terms*— high resolution CT, shape registration, Ricci flow

## 1. INTRODUCTION

Recent papers about cardiac reconstruction using high resolution CT images [4] have shown the complex topological structure of the left ventricle. The interior of the left ventricle surface includes many holes and handles. Papillary muscles are also topologically complicated, as they are “rooted” on the interior surface of the left ventricle. Even if we smooth out the model and basically ignore the complicated trabeculae, there are still a handful of handles left on the base of the papillary muscles. To build a faithful and useful model, the complex structures (especially the papillary muscles), which contain clinically useful information, have to be preserved while modeling for structural and functional analysis.

Establishing point-correspondences that have anatomical meaning is crucial for many applications. For instance, the Active Shape Model (ASM) requires a one-to-one correspondence to get the mean geometry of a shape and some statistical modes of geometric variations [1]. Another example is the patient-specific blood flow simulation, which is a powerful tool for the study of cardiac blood flow and is getting more and more attention in the medical imaging community [9]. The detailed cardiac shape is used as the boundary conditions in a fluid simulator to derive the hemodynamics throughout the whole heart cycle. This simulator also requires that the

cardiac shape must contain the correct one-to-one correspondence among frames to provide the velocity of the boundary in order to drive the simulator.

Existing registration methods are not suitable for this problem. The complicated structure of the left ventricle makes the registration very different from that of some organs such as liver, lung, etc., which are usually modeled with simple topology as genus zero. There are several categories of shape registration algorithms such as, point based methods, including point set registration using Gaussian Mixture Models [6], iterative closest point(ICP) methods [14, 3], optical-flow-like correspondence interpolation [13] and deformable model methods [4, 10]. These shape registration techniques has been widely investigated in biomedical applications [12]. Those methods do not explicitly include topology, thus that there is no guarantee of topology consistency after registration. Some methods could handle the genus zero surfaces, such as a harmonic map [16]. However, the method cannot handle surfaces with arbitrary topology.

For the particular application of high resolution cardiac registration, in [4], Gao et al. proposed a framework that uses high resolution data to reconstruct the 4D motion of the endocardial surface of the left ventricle for a full cardiac cycle. Their method deforms the same mesh model between frames, such that it obtains one-to-one correspondence as a byproduct while reconstructing the left ventricle. The essential method used in their framework is the adaptive focus deformable model(AFDM) [11]. The deformable model deforms in a way that seeks regions with similar geometric structure. While the AFDM model works well in many cases, especially with simple topology, a major drawback is that the AFDM method cannot prevent models from self-intersection. The high genus of the surfaces makes direct registration methods challenging. All the methods mentioned above cannot be applied directly in this scenario.

These challenges, i.e., complex topology and large deformation, motivate us to apply a novel method based on surface Ricci flow. According to the uniformization theorem in differential geometry [7], all surfaces in real life can be flattened onto one of three canonical spaces, the sphere, the plane and the hyperbolic disk, in an angle preserving manner.

Therefore, all geometric problems in three dimensional Euclidean space can be converted to two dimensional problems on the plane. High genus surfaces can be flattened onto the hyperbolic disk. For surface registration, we map both models to their canonical shape; thus, our problem becomes a 2D matching problem which is much easier. Surface Ricci curvature flow is a practical method to compute such types of flattening.

The algorithm proposed is as the followed. For each given heart surface, we first compute the uniformization metric to flatten it onto a Poincaré disk, using discrete hyperbolic Ricci flow [7], then we segment the surface to canonical hyperbolic hexagons, which become convex after they have been transferred into the Klein model [8]. The final step is to compute the harmonic mapping between these convex hyperbolic hexagons. By doing this, we transfer a high genus surface registration problem to a simple convex domain harmonic mapping problem, and guarantee the final mapping between surfaces will be one-to-one (diffeomorphism). We demonstrate the performance of our method in high resolution left ventricle models and compare it with the work in [4].

## 2. THEORETICAL BACKGROUND

In the following, we briefly introduce the background knowledge needed for our method [2].

### 2.1. Surface Ricci Flow

Any closed surface  $S$  satisfies the following Gauss-Bonnet theorem [2]: **Ricci Flow**[5] is a powerful curvature flow method describing a process to deform the Riemannian metric according to curvature, such that the curvature evolves like a heat diffusion process:

$$\frac{dg}{dt} = -2Kg. \quad (1)$$

**Theorem 1 (Uniformization)** *Suppose  $(S, g)$  is an oriented metric surface, then it can be conformally mapped to one of three canonical spaces, the sphere, the plane or the hyperbolic disk, depending on its topology, and with constant Gauss curvature everywhere.*

### 2.2. Hyperbolic Geometry

**Definition 1 (Poincaré disk)** *The Poincaré disk[2] is the unit disk on the complex plane  $\mathbb{D} = \{|z| < 1, z \in \mathbb{C}\}$ , with hyperbolic metric  $ds^2 = \frac{dzd\bar{z}}{(1-z\bar{z})^2}$ .*

Another model of hyperbolic space is the **Klein model**[8]. The following formula converts the Poincaré disk model to the Klein model:  $z \rightarrow \frac{2}{1+z\bar{z}}$ . A pair of topological **pants** is a genus zero surface with three boundaries. A pair of pants is called a pair of **hyperbolic pants**, if it has a hyperbolic metric, and all boundaries are geodesics.

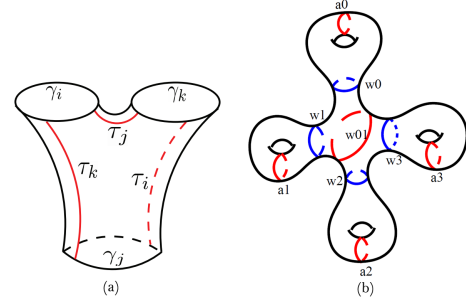


**Fig. 1.** (a): A pair of hyperbolic pants with three geodesic boundaries. (b): A genus  $g$  surface is decomposed to  $2g - 2$  pairs of hyperbolic pants by  $3g - 3$  geodesic cutting loops.

## 3. ALGORITHMS

The main algorithm pipeline is illustrated in Figure 2. The algorithm includes three steps: Discrete Hyperbolic Ricci Flow, Hyperbolic Pants Decomposition and Hyperbolic Hexagon Matching.

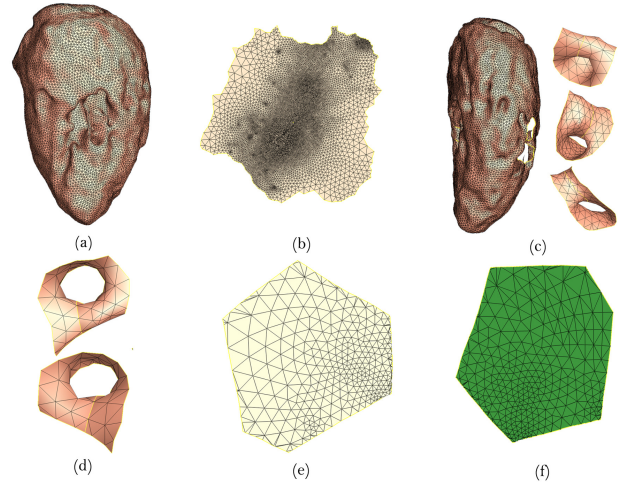


**Fig. 2. Algorithm pipeline:** (a) Original surface  $M_1$ . (b) Compute the uniformization metric of  $M_1$  on the Poincaré disk using discrete hyperbolic Ricci flow. (c) Segment  $M_1$  hyperbolic pants. (d) Further cut each hyperbolic pants into 2 hyperbolic hexagons. (e) The correspondent convex hexagon of the hyperbolic hexagon. (f) The corresponding convex hexagon of another surface  $M_2$  to be registered with  $M_1$ . Building all the mapping between corresponding hyperbolic hexagons, induces the mapping between  $M_1$  and  $M_2$ .

**Step 1: Discrete Hyperbolic Ricci Flow** The computation of the hyperbolic metric on a triangular mesh is based on the discrete hyperbolic Ricci flow [7] [15], as Algorithm 1 shows.

**Step 2: Hyperbolic Pants Decomposition** Given a genus  $g$  closed surface, we compute the hyperbolic pants decom-

---

**Algorithm 1** Discrete Hyperbolic Ricci Flow.

---

**Input:** Surface  $M$ .

**Output:** The hyperbolic metric  $U$  of  $M$ .

1. Assign a circle at vertex  $v_i$  with radius  $r_i$ ; For each edge  $[v_i, v_j]$ , two circles intersect at an angle  $\phi_{ij}$ , called edge weight.
2. The edge length  $l_{ij}$  of  $[v_i, v_j]$  is determined by the hyperbolic cosine law:  $\cosh l_{ij} = \cosh r_i \cosh r_j + \sinh r_i \sinh r_j \cos \phi_{ij}$
3. The angle  $\theta_i^{jk}$ , related to each corner, is determined by the current edge lengths with the inverse hyperbolic cosine law.
4. Compute the discrete Gaussian curvature  $K_i$  of each vertex  $v_i$ :

$$K_i = \begin{cases} 2\pi - \sum_{f_{ijk} \in F} \theta_i^{jk}, & \text{interior vertex} \\ \pi - \sum_{f_{ijk} \in F} \theta_i^{jk}, & \text{boundary vertex} \end{cases} \quad (2)$$

where  $\theta_i^{jk}$  represents the corner angle attached to vertex  $v_i$  in the face  $f_{ijk}$

5. Update the radius  $r_i$  of each vertex  $v_i$ :  $r_i = r_i - \epsilon K_i \sinh r_i$
  6. Repeat the step 2 through 5, until  $\|K_i\|$  of all vertices are less than the user-specified error tolerance.
- 

position which decomposes the original surface into  $2g - 2$  hyperbolic pants. We compute a set of loops  $\{l_1, l_2 \dots l_{3g-3}\}$  that topologically cut  $M$  into  $2g-2$  pants. And then compute a set of geodesics loops  $\{\bar{l}_1, \bar{l}_2 \dots \bar{l}_{3g-3}\}$  that they are homotopic to  $\{l_1, l_2 \dots l_{3g-3}\}$ . These geodesics loops can decompose  $M$  into  $2g-2$  hyperbolic pants.

For a closed surface, each homotopy class has a unique geodesic loop under a hyperbolic metric; the hyperbolic cut loops form a canonical segmentation of the surface, so it is intrinsic to enforce the corresponding hyperbolic hexagons boundaries geodesics to be matched in Hyperbolic Hexagon Matching subsection.

**Step 3: Hyperbolic Hexagon Matching** We carried out the matching between hyperbolic hexagons using harmonic mapping. It is well known that if the target mapping domain is convex, the harmonic map will be a diffeomorphism. So we first transfer the hyperbolic hexagon into the Klein model, in which the hyperbolic hexagon is mapped to a convex Euclidean polygon. This step guarantees the final registration between heart surfaces is one-to-one. Details can be found in Algorithm 2.

#### 4. EXPERIMENTAL RESULTS AND VALIDATION

We applied our heart surface registration method to a sequence of high resolution left ventricle models. The models are 10 frames of heart surfaces segmented from CT volumes. The CT data were acquired on a  $320 - MDCT$  scanner using a conventional ECG-gated contrast-enhanced

---

**Algorithm 2** Hyperbolic Hexagon Matching Algorithm.

---

**Input:** Two hyperbolic hexagons  $H_1$  and  $H_2$ .

**Output:** The harmonic mapping between  $H_1$  and  $H_2$ .

1. Compute hyperbolic mappings which map the  $H_1$  and  $H_2$  onto the Poincaré disk. As we already have the uniformization metric of the original surface and the cut loops, this step can be done by simply cutting the uniformization domain mesh along the pants decomposition cuts loops (we name the corresponding uniformization domain meshes  $U_1$  and  $U_2$ ).
  2. Convert  $U_1$  and  $U_2$  from the Poincaré disk model to the Klein model; then  $U_1$  and  $U_2$  become convex polygons.
  3. Compute a harmonic map between  $U_1$  and  $U_2$ , then construct a mapping between original  $H_1$  and  $H_2$  using the mapping between  $H_i$  and  $U_i$ ,  $i \in \{1, 2\}$ .
- 

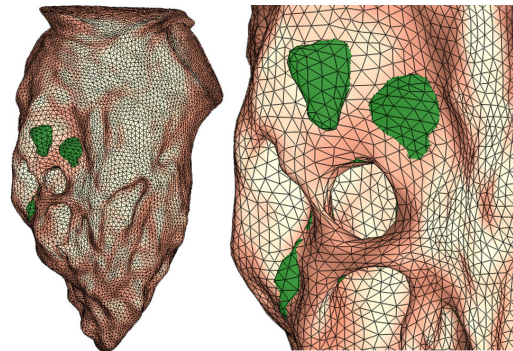
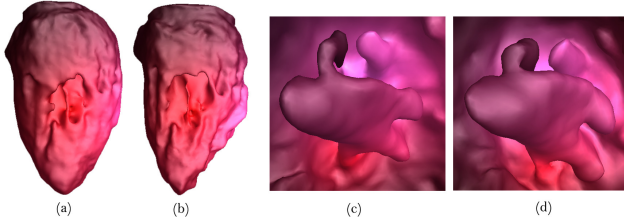


**Fig. 3.** The model after registration in [4], which deforms the source model to the target model. The method cannot prevent self-intersections shown by the green regions, which are part of the papillary muscle inside of the left ventricle and have been deformed to the outside of the left ventricle.

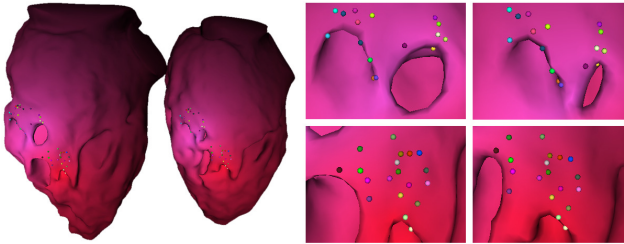
CT angiography protocol. The imaging protocol parameters include: prospectively triggered, single-beat, volumetric acquisition; detector width  $0.5mm$ , voltage  $120KV$ , current  $200 - 550mA$ . Reconstructions were done at 10 equally distributed time frames in a cardiac cycle. The resolution of each time frame is  $512$  by  $512$  by  $320$ . The left ventricle models are reconstructed using the method described in [4]. Although their methods already provide one-to-one correspondence during reconstruction, the registration quality is not reliable. Most importantly, their method cannot prevent self intersection, as shown in Figure 3.

Figure 4 shows a colormap of the registration results. The points with the same color correspondent to each other. The results show reliable registration between frames. Figure 5 shows detailed point-to-point correspondence around handles, which is a challenging part of the model. The same color points correspond to each other. The proposed methods guaranteed the one-to-one correspondence and topology consistency.

We evaluated the accuracy of the matching results  $\phi : S_1 \rightarrow S_2$  by using the shape error defined in [15], namely



**Fig. 4.** ColorMap for Registration results: the points which have the same color correspond to each other. Figure (a) and (b) show the registration in front view, figure (c) and (d) show a view of the papillary muscle correspondence inside the heart.



**Fig. 5.** Detailed point to point correspondent: the tiny balls on two registered surfaces with the same color are corresponding points.

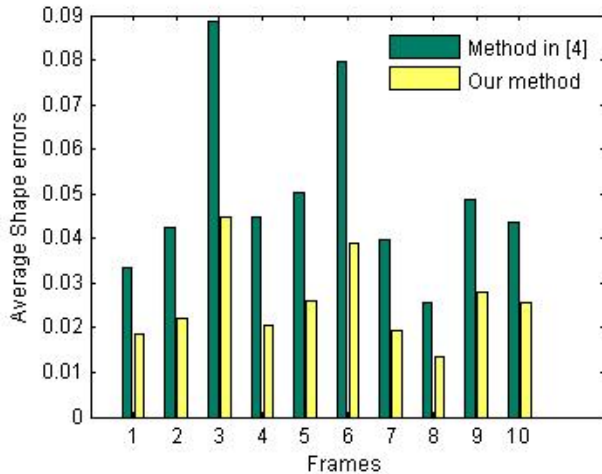


**Fig. 6.** This figure shows the shape error. Each frame is registered to the following frame. The last frame is registered to the first one.

the average distance between the source point and the corresponding image point, normalized by the diagonal of the bounding box of the target surface. Figure 6 shows the shape error. Both methods are tested on desktop Intel Core2 Quad Q6600 2.4GHz. The proposed method is more efficient for registering two models (20,000 vertices for each model) in around 35" other than 8'30" in [4].

## 5. CONCLUSIONS

We have proposed a novel method to register the left ventricle endocardial surface models. The complicated structures inside the left ventricle, such as the papillary muscles, are preserved during registration. Our method guaranteed the one-to-one correspondence and the shape topology consistency.

## 6. ACKNOWLEDGMENTS

This material is based upon work supported by the National Institutes of Health under Grant No.R21HL88354-01A1, Multiscale Quantification of 3D LV Geometry from CT.

## 7. REFERENCES

- [1] T. F. Cootes, C. J. Taylor, D. H. Cooper, and J. Graham. Active shape models-their training and application. *CVIU*, 61:38–59, January 1995.
- [2] M. P. do Carmo. *Riemannian Geometry*. Prentice Hall, 1992.
- [3] M. Erdmann, E. G. Mit, D. A. Simon, and D. A. Simon. Fast and accurate shape-based registration. Technical report, 1996.
- [4] M. Gao, J. Huang, S. Zhang, Z. Qian, S. Voros, D. N. Metaxas, and L. Axel. 4D cardiac reconstruction using high resolution CT images. In *FIMH*, pages 153–160, 2011.
- [5] R. Hamilton. The ricci flow on surfaces. *Mathematics and General Relativity*, 71:237–262, 1988.
- [6] B. Jian and B. C. Vemuri. Robust point set registration using gaussian mixture models. *PAMI*, 33(8):1633–1645, 2011.
- [7] M. Jin, J. Kim, and X. D. Gu. Discrete surface ricci flow: Theory and applications. In *IMA Conference on the Mathematics of Surfaces*, pages 209–232, 2007.
- [8] M. Jin, F. Luo, and X. D. Gu. Computing surface hyperbolic structure and real projective structure. *SPM '06*, pages 105–116, 2006.
- [9] S. Kulp, M. Gao, S. Zhang, Z. Qian, S. Voros, D. N. Metaxas, and L. Axel. Using high resolution cardiac CT data to model and visualize patient-specific interactions between trabeculae and blood flow. In *MICCAI (1)*, pages 468–475, 2011.
- [10] J. Montagnat and H. Delingette. 4D deformable models with temporal constraints: application to 4D cardiac image segmentation. *MEDIA*, 9(1):87 – 100, 2005.
- [11] D. Shen and C. Davatzikos. An adaptive-focus deformable model using statistical and geometric information. *PAMI*, pages 906–913, 2000.
- [12] I. A. Sigal, M. R. Hardisty, and C. M. Whyne. Mesh-morphing algorithms for specimen-specific finite element modeling. *Journal of Biomechanics*, 41(7):1381 – 1389, 2008.
- [13] A. Tevs, M. Bokeloh, M. Wand, A. Schilling, and H.-P. Seidel. Isometric registration of ambiguous and partial data. In *CVPR*, pages 1185 –1192, 2009.
- [14] K. Wilson, G. Guiraudon, D. L. Jones, and T. M. Peters. 4D shape registration for dynamic electrophysiological cardiac mapping. In *MICCAI (2)*, pages 520–527, 2006.
- [15] W. Zeng, D. Samaras, and X. D. Gu. Ricci flow for 3D shape analysis. *PAMI*, 32(4):662–677, 2010.
- [16] D. Zhang and M. Hebert. Harmonic maps and their applications in surface matching. In *CVPR*, pages 2524–2530, 1999.